Extended x-ray-absorption fine-structure study of the Jahn-Teller phase transitions in $CsCrCl_3$ and $RbCrCl_3$ hexagonal perovskites

S. Gota, J. García, J. Chaboy, and J. Bartolomé
Instituto de Ciencia de Materiales de Aragón, Consejo Superior de Investigaciones Científicas–Universidad de Zaragoza, 50009 Zaragoza, Spain
(Received 1 March 1991)

The local structure of the ($CrCl_6$) complex, in the different phases of $CsCrCl_3$ and $RbCrCl_3$ compounds, is determined by means of the extended x-ray-absorption fine-structures technique. It is proved that the complexes are distorted (elongated) in the high-temperature symmetrical ($P6_3/mmc$) α phase and in the intermediate ($C2/m$) β phase present in $RbCrCl_3$. The disortion amounts to $\rho_0=0.39$ Å at all temperatures. These results clarify the validity of the different conjectures on the possibility of distortion in the α phase derived from different experimental techniques.

I. INTRODUCTION

Some structural phase transitions in solids are due to the coupling of the electronic states of the constituent atoms to the nuclear motion of the lattice. The electronic ground-state degeneracy (non-Kramers) of highly symmetrical (nonlinear) molecules or complexes is broken by a distortion stabilizing a lower symmetry (Jahn-Teller effect, JT).[1,2] If the active JT ions are in large concentration, these local instabilities induce macroscopic phase transitions when the temperature decreases, corresponding to the different arrangements of the distorted complexes. This is the cooperative Jahn-Teller transition (CJTT).

The present paper deals with $ACrCl_3$ (A=Rb, Cs) hexagonal perovskites which fulfill the above-mentioned conditions. These compounds belong to the family of hexagonal perovskites $ABCl_3$ (Refs. 3–5) (A=Rb, Cs, $B=3d$ transition metal) which generally have the $BaNiO_3$ structure (space group $P6_3/mmc$). Its structure is formed by linear chains of face sharing octahedra (BCl_6) along the c axis, separated by the A atoms, as shown in Fig. 1. A characteristic of this family is the absence of any structural phase transition unless B is Cr^{2+} or Cu^{2+}, i.e., when both ions are JT active, providing good examples of CJTT.[6,7]

From x-ray-diffraction data it is known that the two Cr^{2+} compounds have the same high-temperature α phase ($P6_3/mmc$) and undergo structural phase transitions as the temperature is reduced. $CsCrCl_3$ presents a first-order phase transition at $T_c=171.1$ K to the monoclinic γ phase ($C2$).[3,4,6] On the other hand, $RbCrCl_3$ undergoes a second-order transition from the α phase to an intermediate monoclinic β phase ($C2/m$) at $T_{c_1}=470$ K, before transforming to the common low-temperature γ phase at $T_{c_2}=193.3$ K.[6,8] The transition temperatures and space groups of these compounds, and those of $RbCuCl_3$ and $CsCuCl_3$ for comparison purpose, are summarized in Fig. 2.

In the high-symmetry α phase, the Cr^{2+} ions are placed in octahedral sites of C_{3v} symmetry. Since, in this case, the electronic ground state is an E doublet, the Jahn-Teller electron-vibration $E\times\varepsilon$ coupling stabilizes distorted states of the ($CrCl_6$) complex. The distortion is described in terms of the normal-mode coordinate parameters defined as

$$Q_2=\tfrac{1}{2}(X-Y)=\rho_0\sin\phi \tag{1}$$

and

$$Q_3=\frac{1}{\sqrt{12}}(2Z-X-Y)=\rho_0\cos\phi$$

X, Y, and Z, respectively, are the distances between the Cl^- ions along the three diagonals of the octahedron, and ρ_0 and ϕ represent the same states in polar coordinates. The energy surface of the distorted states configurates the so-called "Mexican hat," $U(\rho,\phi)$, which presents a

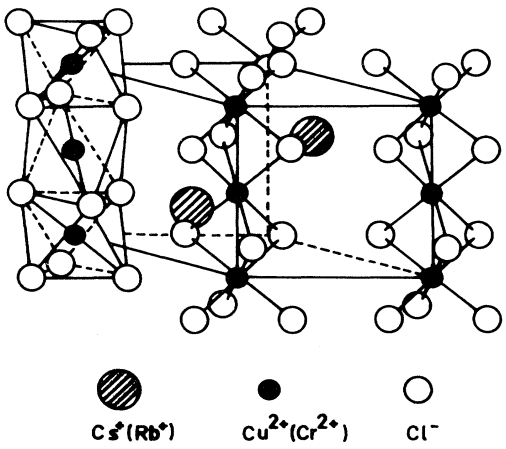

FIG. 1. Crystallographic structure of the hexagonal perovskites $RbCrCl_3$ and $CsCrCl_3$. At the left of the picture, the phase-sharing octahedra chain structure along the (0,0,1) direction is drawn.

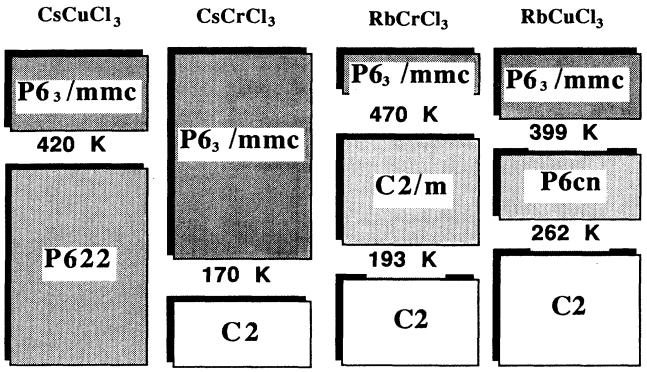

FIG. 2. Crystallographic space groups and transition temperatures of the family $ABCl_3$; A=Rb,Cs, B=Cr,Cu, for the α, β, and γ phases.

trough with a minimum-energy value E_{JT}, the Jahn-Teller stabilizing energy, for the stable distortion ρ_0 [the first two terms of formula (2)].

Originally[9] it was considered that the mechanism for the CJTT was that, in the high-temperature phase, the octahedra were regular and highly symmetric, while it was the lowering of temperature that caused the individual octahedra to distort simultaneously at the onset of the phase transition. Today it is known that this is only the case when the energy E_{JT} is of the order of the transition temperature.

However, if E_{JT} is larger than the range of temperature of interest, then the nonlinear anharmonic coupling yields the so-called "warping energy term," β, of the "Mexican hat" to be added to the first two terms:

$$U/E_{JT}=-2\left[\frac{\rho}{\rho_0}\right]+\left[\frac{\rho}{\rho_0}\right]^2-\frac{\beta}{E_{JT}}\left[\frac{\rho}{\rho_0}\right]^3\cos 3\phi\ . \qquad (2)$$

It gives rise to three states of minimum energy corresponding to distortions along the three diagonals of the octahedron (elongations for $\beta>0$). The energy barrier hindering the transitions between the three minima is 2β. If β is small, elongations as well as contractions will be present. On the contrary, if β is large, only elongated octahedra will appear. The three possible elongations of the octahedron along the diagonals are represented by the values of $\phi=0,\pm 2\pi/3$.

Thus, for β large, the high-symmetry α phase is considered to be formed by distorted octahedra with the elongated axis distributed along the chain randomly in space or time over the three possible orientations for each octahedron. We can distinguish two regimes of temperature: In the "dynamical regime" (at temperatures of the order of β) the thermal disorder allows each octahedron to change its distortion between the three equivalent ground states, i.e., elongation of one out of the three diagonals. In the "static regime" (low temperature with respect to β), the thermal-activated jumps among the three distortions are quenched and one only finds distorted octahedra. The structure is then fixed and ordered. Some experiments mentioned below are compatible with the description of nonlinear Jahn-Teller coupling in the dynamical regime.[10]

From the x-ray-diffraction data, Crama[5] has noticed that the c/a ratio does not differ significantly in the α, β, and γ phases. This is in agreement with the dynamical picture of distorted octahedra in the α phase and could be expected if distorted octahedra were present in all phases. Also, a highly anisotropic thermal motion of the Cl^- ions was derived when they considered the α phase to be formed by regular octahedra.

As a consequence, to interpret the high-temperature α-phase diffraction data obtained on single crystals of $CsCrCl_3$ and $CsCrI_3$, several models were proposed:[3] (a) four with space symmetry $P6_3/mmc$; i.e., one static model of a high-symmetrical ordered phase, and three disordered models considering twofold, threefold, or fourfold positional disorder for each Cl^- position, respectively, (b) one with space symmetry $P6_3mc$, which had been proposed earlier.[11] It was concluded that the best refinements were obtained for the $P6_3/mmc$ disordered models, but no best choice between them could be reached. Then the authors conjecture that the octahedra are distorted in the α phase and, moreover, three different Cr-Cl distances are given (see Table I) amounting to an elongation of $\rho_0=0.34$ Å. For $CsCrI_3$, the value of 0.32 Å was found. The α phase of $CsCuCl_3$ has been interpreted within the same model and the distortion proposed is $\rho_0=0.43$ Å.[12]

The β phase of $RbCrCl_3$ is described by a sequence of alternating compressed (XY) and elongated (Z) ocatahedra. Actually, the compressed octahedra are also conjectured to be disordered between two possible elongated axes.[8] Four different Cr sites are proposed, the two elongated octahedra with $\rho_0=0.30$ Å and the averaged distortion of the XY one amounting to $\rho_0=0.22$ Å.

The lowest-temperature phase (γ phase) presents four different octahedra, each of them tetragonally elongated along one of its diagonals.[4,8] The average distortion is reported to be $\rho_0=0.37$ Å both for the Cs and Rb compounds. This phase is characterized by an ordered sequence along the chain of the elongated diagonal of each octahedra.

From the thermodynamic study of the phase transitions,[7] the order-disorder character of the γ-α phase transition of $CsCrCl_3$ was checked, finding 78% of the expected entropy for a high-temperature phase model in which each octahedron may choose between two possible distortions. The assumption that two adjacent octahedra may never have their elongated diagonals meeting at the same corner seems to be fulfilled, as proposed from the x-ray work.[4]

The VIS-NIR spectra of $CsCrCl_3$ and $RbCrCl_3$ (Refs. 11 and 13) pointed in the same direction. The ligand-field A_{1g}-B_{1g} electronic transition found at $\Delta E=6500$ cm^{-1} is associated with an elongated octahedra. However, the transition at 5000 cm^{-1} expected for compressed octahedra in the β phase of $RbCrCl_3$ is not found. The spectra

do not change at the γ, β- and α-phase transitions, which could imply that, in the α phase, elongated octahedra also exist. Moreover, since $\Delta E = 4E_{JT}$, one obtains an estimate of the JT stabilizing energy of about 2400 K. This is a bit lower, but of the same order of magnitude as for $CsCuCl_3$ where $E_{JT} = 3000$ K (Ref. 14) and, consequently, both may be considered as strong Jahn-Teller coupled systems.

TABLE I. Parameters used to simulate the theoretical EXAFS fits shown in Figs. 4 and 5 for the different phases of $CsCrCl_3$ and $RbCrCl_3$. σ^2 is the EXAFS Debye-Waller exponent, F is the fitting index defined in the text. Interatomic distances from EXAFS and from x-ray-Diffraction data are collected. The third (less significant) decimal is given in parentheses.

		$CsCrCl_3$		
Phase number of bonds	R (Å) XRD	R (Å) EXAFS	σ^2 (Å^2)	F
γ	$T=60$ K[a]	$T=10$ K		
	$\rho_0=0.37(5)$	$\rho_0=0.38(7)$		
2×Cr-Cl	2.36(6)	2.35(6)	0.006	0.868
2×Cr-Cl	2.47(0)	2.42(9)	0.007	
2×Cr-Cl	2.74(4)	2.72(2)	0.007	
2×Cr-Cr	3.08(5)	3.06(5)	0.016	
γ		$T=100$ K		
		$\rho_0=0.40(8)$		
2×Cr-Cl		2.36(0)	0.011	0.261
2×Cr-Cl		2.42(8)	0.010	
2×Cr-Cl		2.71(9)	0.013	
2×Cr-Cr		3.09(6)	0.022	
α	$T=295$ K[b]	$T=230$ K		
	$\rho_0=0.34(5)$	$\rho_0=0.39(4)$		
2×Cr-Cl	2.44(7)	2.33(6)	0.015	0.438
2×Cr-Cl	2.50(6)	2.42(4)	0.015	
2×Cr-Cl	2.64(0)	2.71(4)	0.018	
2×Cr-Cr	3.11(9)	3.07(2)	0.026	
		$RbCrCl_3$		
Phase number of bonds	R (Å) XRD	R (Å) EXAFS	σ^2 (Å^2)	FI
γ	$T=100$ K[a]	$T=116$ K		
	$\rho_0=0.37(4)$	$\rho_0=0.39(8)$		
2×Cr-Cl	2.38(5)	(2)2.35(6)	0.008	0.868
2×Cr-Cl	2.44(6)	(2)2.43(0)	0.008	
2×Cr-Cl	2.73(5)	(2)2.73(2)	0.010	
2×Cr-Cr	3.11(9)	(2)3.11(6)	0.029	
β	$T=295$ K[a,c]	$T=300$ K		
	$\rho_{0(1)}=0.30(4)$	$\rho_0=0.39(8)$		
2×Cr_1-Cl	2.40(3)	(2)2.35(6)	0.014	0.174
4×Cr_1-Cl	2.59(2)	(2)2.43(1)	0.014	
		(2)2.73(1)	0.017	
	$\rho_{0(2)}=0.22(4)$			
4×Cr_2-Cl	2.40(3)			
2×Cr_2-Cl	2.69(2)			
2×Cr-Cr	3.12(3)	(2)3.12(0)	0.050	

[a]W.J. Crama *et al.*, Acta Crystallogr. B **35**, 1875 (1979).
[b]W. J. Crama and H. W. Zandbergen, Acta. Crystallogr. B **37**, 1027 (1980).
[c]W. J. Crama *et al.*, Acta Crystallogr. B **34**, 1973 (1978).

More recently, quasielastic diffuse neutron scattering has been performed on the $CsCuCl_3$ compounds.[15] They conclude that the anisotropic diffuse scattering observed near the Bragg peaks may be interpreted in terms of the "density impurity" Huang scattering due to the JT individually distorted octahedra, each acting as an impurity center. At high temperature they are independent from the neighboring complexes, acting as defects. In a more developed analysis of their data they conclude that some dynamic correlation is present in the high-temperature phase, interpreting their data within an elastic-dipole interactions model.[16]

Also on the $CsCuCl_3$, the temperature dependence of the EPR linewidth across the phase transition was interpreted in terms of the exchange modulation of the Dzyaloshinsky-Moriya antisymmetric interaction, and proposed that, in the high-temperature α phase, the octahedra were distorted, with a relaxation time of the distortion much longer than 10^{-12} sec.[17]

Given all these antecedents on the Cr and Cu hexagonal perovskites, it seemed a sound idea to use the extended x-ray-absorption fine-structure (EXAFS) technique to prove the conjecture of the existence of distorted octahedra in the α phase, and probably in the β phase of the $RbCrCl_3$ as well.

This technique is ideal since it gives information about the local structure even when there is no long-range order (in our case, when the octahedra are not sequentially ordered). Jahn-Teller-induced distortions of octahedra have been previously studied in Cu^{2+} clusters proving to be a resolutive technique.[18] But the crucial point in the present case is the characteristic time of the photoelectric process (10^{-16} sec),[19,20] much shorter than the jump inverse frequency (10^{-11}–10^{-13} sec) related to the permanence time in each of the distorted states in the dynamical JT regime. In this way, we can obtain an "instant picture" of the ($CrCl_6$) octahedra and verify whether the individual octahedra are distorted in all phases.

II. EXPERIMENT

X-ray-absortion spectra at the Cr K edge were measured in the transmission mode at the INFN Frascati Synchrotron Facility on the PULS EXAFS station. The spectra have been recorded at different temperatures ($T=10$, 100, and 230 K for $CsCrCl_3$ and $T=116$ and 300 K for $RbCrCl_3$) corresponding to the different crystallographic phases. Samples were prepared by spreading powder on a kapton tape attached to a thick aluminum foil to maintain the thermal homogeneity. The same samples used in previous calorimetric studies[7] have been used here.

The background subtraction of the experimental EXAFS signal was performed with standard methods:[20] the program EXBACK (Ref. 21) and the package programs from PULS (Ref. 22) and Zaragoza[23] have been used. EXAFS simulations were carried out applying the code EXCURV88,[24] which is based upon the spherical wave theory developed by Lee and Pendry[25] incorporating the fast curved-wave method[26] to reduce the computational time needed.

The magnitude of the x-ray-absorption fine structure, $\chi(k)$, is given by

$$\chi(k)=\sum_i \frac{N_i}{kR_i^2}\sin(2kR_1+2\delta+\psi_i)|f(\pi)| \times e^{-\sigma_i^2k^2}e^{-2\Sigma_{\mathrm{Im}}R_i/k} .$$

The summation is over the number of shells contributing to the EXAFS and k is the photoelectron wave vector. N_i is the coordination number and R_i the interatomic distance for the ith shell; δ and ψ_i are phase shifts experienced by the photoelectron; σ_i^2 is the Debye-Waller factor and Σ_{Im} is the imaginary part of the photon-electron self-energy, accounting for inelastic scattering. $|f(\pi)|$ is the amplitude of the photoelectron backscattering factor.

The quality of the theoretical simulations was assessed by visual comparison of the experimental and simulated EXAFS spectra and their Fourier transforms, and by calculation of the fitting index defined, in the program EXCURV88, as follows:

$$F=\frac{1}{(100N_p)}\sum_{i=1}^{N_p}(\mathrm{Res}_i kW)^2 ,$$

where Res_i = residual $i=\chi_i(\mathrm{calc})-\chi_i(\mathrm{expt})$ and N_p = number of data points. W is an integral weight which is used to offset the decay of χ as the energy increases. Also, phase shifts are more accurate at high k and errors in defining the energy zero, represented in EXCURV88 by the parameter E_0, are also less significant.

Atomic phase shifts and backscattering factors were calculated approximating the excited chromium atom to the neutral manganese atom with one electron removed from the 1s level ($Z+1$ approximation). Throughout the analysis, k-cubed weighting was applied to compensate for the diminishing amplitude at high k and to determine the experimental spectrum shift, $E_0=8.71$ eV, needed to match the theoretical simulation.

III. RESULTS

The data analysis was begun with the low-temperature static phases, in which the Cr-Cl distances of the ($CrCl_6$) octahedra have been well characterized by x-ray diffraction. This allows us to fix, during the analysis of the high-temperature phase, E_0, Σ_{Im}, and the empirical correction for photoelectron shakeup and shakeoff, AFAC, strongly correlated with the structural parameters. In this way, the only parameters that have been allowed to vary in the refinement process are the interatomic distances and the Debye-Waller factors.

Fourier transforms for both compounds, $RbCrCl_3$ and $CsCrCl_3$, recorded at different temperatures, are shown in Fig. 3. It is clear from this figure that, in both cases, the most important contribution to the EXAFS signal comes from the high and wide peak centered at $R=2.40$ Å. We identify it as due to the Cl^- environment around the Cr^{2+} emitter ion, the small shoulder on the right side being related with the contribution of the two Cr^{2+} ions be-

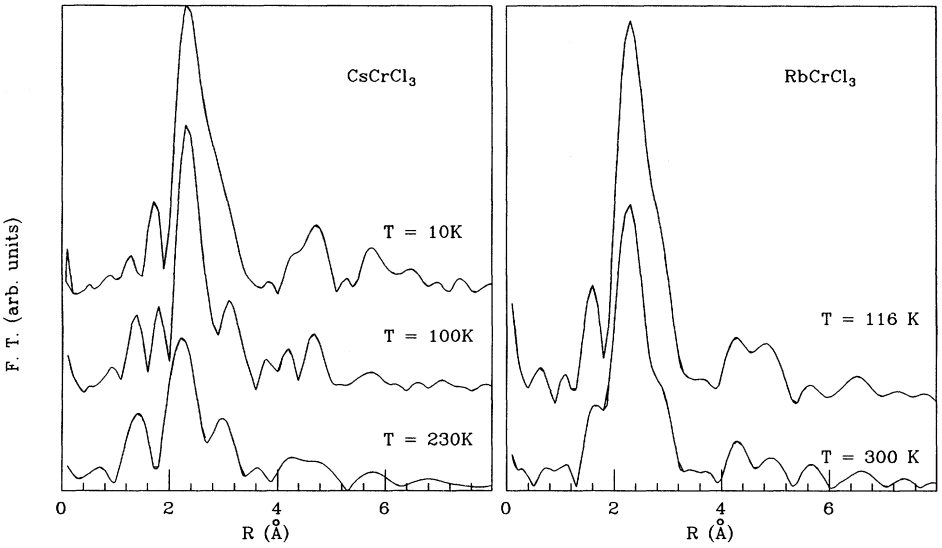

FIG. 3. Modulus of the Fourier transform of the experimental EXAFS spectra at temperatures corresponding to their different crystallographic phases of $CsCrCl_3$ (left) and $RbCrCl_3$ (right).

longing to the adjacent octahedra. The height of the modulus of the Fourier transform decreases as the temperature increases. This effect originates from the larger thermal atomic motion at higher temperatures. Consequently, the interference between the two shells varies as well, and is reflected by the change in shape and position of the shoulder.

In order to determine the local structure around the chromium atom for the high-temperature phases in both compounds, $CsCrCl_3$ and $RbCrCl_3$, the EXAFS signal was Fourier filtered in the range $R=0-3.5$ Å, where the chromium and chlorine atoms contribution cannot be separated. At the same time, this procedure removes the complications on the theoretical simulation arising from

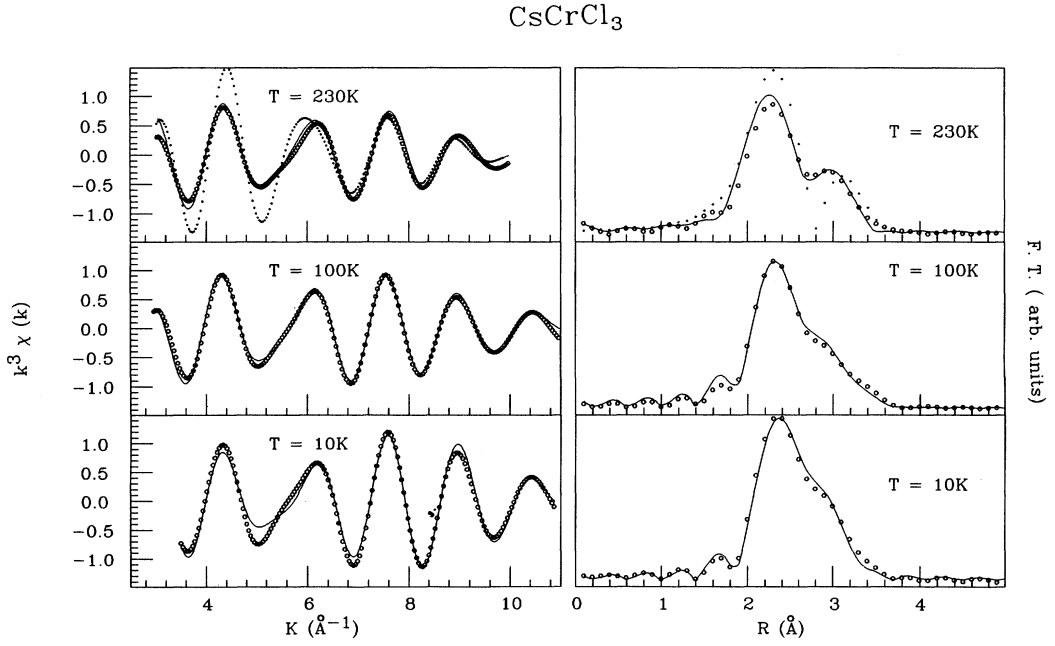

FIG. 4. EXAFS (left) and Fourier transform (right) of the K^3-weighted simulation of the first shell of $CsCrCl_3$. The solid line corresponds to the best fit for elongated octahedra with $\rho_0=0.39$ Å. The dotted line in the $T=230$-K results (α phase) represents the prediction for regular octahedra.

the existence of non-negligible multiple-scattering contributions beyond the second coordination shell in such a class of structures.[27]

The structural parameters, obtained from the fit to the theoretical simulations, are summarized in Table I where, together with the coordination numbers, interatomic distances and Debye-Waller exponents, σ^2, are shown. For comparison purposes, the results obtained from crystallographic studies are included. Except for the $RbCrCl_3$ β phase, the short, intermediate, and long Cr-Cl distances are given. They are averaged over the different Cr sites in the γ phase.

The comparison between the calculated EXAFS signals and the experimental Fourier-filtered spectra for the $RbCrCl_3$ and $CsCrCl_3$ compounds at the low-temperature γ phase ($T=10$ and 100 K for the Cs and $T=116$ K for the Rb compound) are shown in Figs. 4 and 5. The best fits have been obtained when we include as input parameters three chlorine shells, two of them corresponding to the short distances of the distorted octahedron and the other one to the long distance. The splitting of the short distances into two is necessary to obtain the convergence of the fitting process.

The fit is quite satisfactory, only for the $T=10$-K case is a discrepancy in the $k=4.5-5.8$ Å^{-1} range present. In any case, the fit indexes are better than those currently accepted.[28] From Table I we can infer by inspection that the only significant change between the parameters for the 10- and 100-K fits amounts to a slight decrement of the Deby-Waller factor at the lower temperature, as could be expected because of the decrease of the thermal disorder.

The general good agreement between the experimental signals and their theoretical simulations is enough to conclude the correctness of the results. However, in order to be sure about the interference phenomena associated with the existence of two adjacent chromium atoms, we have applied the difference EXAFS data analysis technique[29] to the $CsCrCl_3$ spectrum for $T=10$ K. Thus, for fixed nearest-neighbor Cr-Cl distances, the spectrum was calculated and subtracted from the experimental signal and the remaining signal could be accounted for by the adjacent Cr ions unambiguously.

The results of the analysis for the high-temperature phases α-$CsCrCl_3$ and β-$RbCrCl_3$ are shown in Figs. 4 and 5 too. For the α phase of $CsCrCl_3$, we have tried to fit with two different simulated clusters: one with the same distortions as in the γ phase and another one with six equal Cr-Cl distances (undistorted octahedra). The latter choice gave aberrant results, so beyond any ambiguity we can disregard the possibility of having highly symmetric octahedra and, then, confirm the models proposing disorder. In fact, the best fit was found for interatomic distances very close to those found for the γ phase in this work, i.e., with an elongated axis and two short ones, each different from one another.

For the β phase of $RbCrCl_3$, the best fit has been found for the same distorted octahedra. Again, the bond lengths are very close to the distances found for the γ phase of $RbCrCl_3$ (see Table I). This proves that the so-called X-Y compressed octahedra mentioned in the x-ray work are actually disordered elongated octahedra, as proposed by Crama and Zandbergen.[3]

The Debye-Waller factor obtained with EXAFS consists of two contributions due to the radial motion of the central atom and the Cl atom to which the displacement-displacement correlation function has to be subtracted. Each of the first two terms corresponds to

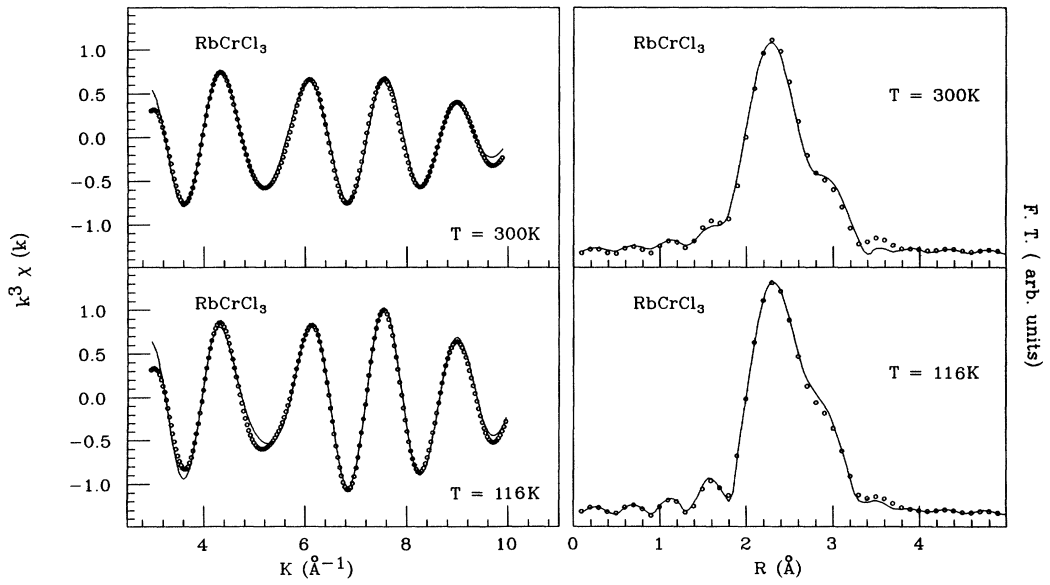

FIG. 5. EXAFS and Fourier transform of the K^3-weighted simulation of the first shell of $RbCrCl_3$.

the monoatomic Debye-Waller factor obtained from x-ray diffraction, so the EXAFS one will always be smaller than the sum of the x-ray ones.[20] For example, for the γ phase of $RbCrCl_3$, the σ^2_{Cr} and σ^2_{Cl} have been determined with x-ray diffraction at 100 K,[5] both amounting to an averaged value of 0.01 Å^2. The EXAFS Debye-Waller σ^2 value should then be less than 0.02 Å^2 and, indeed, we find it to be 0.008 for one Cr-Cl distance and 0.01 for the other. In any case, this analysis tells us that our resulting σ^2 are reasonable.

IV. CONCLUDING REMARKS

The results of the present work are straightforward; in the time scale of the photon-lattice interaction, the octahedra are similarly distorted in the α, β and γ phases. In fact, the distortions amount to $\rho_0 \simeq 0.39$ for all phases and both compounds, in good agreement with the x-ray data for the γ phase.

On the other hand, although our result now confirms the conjecture of distorted octahedra in the α phase,[3] they show that the distortion is greater than that derived from the x-ray-diffraction fits ($\rho_0=0.34$). This result revalidates the same conclusion drawn from the independence of the VIS-NIR spectroscopic data upon temperatures across the phase transitions.

The emerging picture is that, for each octahedron, $E_{JT}=1625$ cm^{-1} (2400 K), and the complex characteristic internal stretching mode which transforms as E_{1g}, responsible for the JT coupling, related to E_{JT} yields to

$$\hbar\omega_0=\frac{\hbar}{\rho_0}\left[\frac{2E_{JT}}{\mu}\right]^{1/2}=142.5\text{cm}^{-1}$$

for $\rho_0=0.39$ Å, and μ is the Cl^- atom mass. This value is slightly higher than $\hbar\omega_0=120$ cm^{-1} deduced for the CsCuCl compound ($E_{JT}=3000$ K), for a distortion of $\rho_0=0.43$ Å, and both are quite similar to the measured E_{1g} Raman-active frequency of $CsNiCl_3$,[30] $\hbar\omega_0=150$ cm^{-1}. From these values one estimates the ratio $E_{JT}/\hbar\omega_0 \approx 11-13$, for the Cr and Cu compounds, respectively. It is high enough to guaranty that the strong-JT coupling limit is valid in both series of compounds.

To place on a better footing our argument that the photon-lattice interaction time is much shorter than the residence time in one of the distortions, dynamical data should be used. The only available data for Cr^{2+} were obtained from acoustical measurements in $KMgF_3:Cr^{2+}$, in which the values of the hindering barrier across different distortions were derived, $2\beta=1000-173$ K, depending on the choice of $\hbar\omega_0$ (400–300 cm^{-1}, respectively).[31] Such a wide range is of little help, so we shall refer to the better-studied $CsCuCl_3$ compound.

As mentioned in the Introduction, from EPR measurements, a lower limit to the distortion relaxation time in this latter compound is 10^{-12} sec.[17] On the other hand, in a recent work the neutron quasielastic and inelastic data for $CsCuCl_3$ have been interpreted in terms of the octahedra acting as distortive centers, equivalent to elastic dipoles.[16] From the dynamical point of view, the crucial parameter obtained from the neutron work was the inverse average time a dipole stays in one site, which was found to be $\gamma k_B T=0.14$ meV at 428 K; that is, a permanence time of 3×10^{-11} sec in a given distorted state. An Arrhenius law held for the linewidth of the quasielastic peak as a function of temperature, and from it the value $2\beta=450$ K was deduced.

So, accepting the similarity between the Cu and Cr compounds, we may scale the warping term for the Cr compound with the lower E_{JT}, obtaining $2\beta=360$ K. With the parameters measured (E_{JT},ρ_0) and proposed (β), the effective potential surface describing the dynamic JT effect in these compounds has been represented in Fig. 6. Then, the expected permanence time in one distortion will be of the order of $10^{-10}-10^{-11}$ sec, which is much higher than the time scale of our experiment, as we expected. Quasielastic neutron-scattering experiments would probably be necessary to ascertain the value of β. These facts and that E_{JT} is much higher that the experimentally relevant temperatures in this work, suggest that one should expect to observe distorted octahedra at all temperatures, as one actually does.

To explain the long-range ordering in the different phases of these compounds, a three-state Potts model has been proposed,[6,32] each state corresponds to one of the possible elongations of the octahedra. In the α phase each octahedron has just two possible distortions due to the steric condition that two elongated axes may not coincide in the same corner. In the β phase, alternate octahedra jump between two possible elongations. Our results agree with that model and, moreover, indicate that the individual distortion is practically identical in all phases. Then the elastic coupling between local distortions (inter and intrachain) is responsible for the different phase transitions, giving rise to the ordered stable phases.

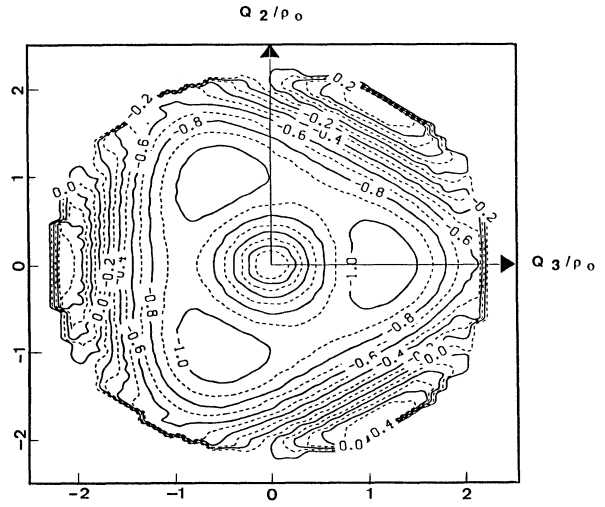

FIG. 6. Contour plot of the energy surface U/E_{JT} for the Jahn-Teller distorted octahedra, with $\rho_0=0.39$ Å, $E_{JT}=2400$ K, and $2\beta=360$ K. The isolines are given in E_{JT} units.

A more complicated model has been proposed[33] where the distortional modes and a pseudospin describing the interaction between the adjacent distorted octahedra were considered as the intrachain short-range-ordering mechanism. With an effective interchain interaction, the different structures observed in the series were accounted for. Two possibilities were considered: in model *A* the warping term was assumed small implying that any distortion, contraction or elongation, would be possible. In model *B*, the warping term is large and the three-Potts model is again reached. Although the first model has the benefit of predicting correctly the second-order character of the α-β phase transition, we think that our results allow one to disregard case *A*.

In conclusion, it has been proved that the ($CrCl_6$) octahedra are distorted in all crystallographic phases. Consequently, the only model adequate to describe the behavior of these compounds is a three-state Potts model.

ACKNOWLEDGMENTS

This work was supported by CICYT, Project No. MAT 88-302. The Cooperation agreement between the CICYT (Spain) and INFN (Italy) for performing the experiments is acknowledged.

[1]H. A. Jahn and E. Teller, Proc. R. Soc. London Ser. A **167**, 22D (1937).
[2]H. A. Abragham and B. Bleaney, *Electron Paramagnetic Resonance of Transition Metal Ions* (Clarendon, Oxford, 1970), p. 792.
[3]W. J. Crama and H. W. Zandbergen, Acta Crystallogr. B **37**, 1027 (1980).
[4]W. J. Crama, W. J. A. Maaskant, and G. C. Verschoor, Acta Crystallogr. B **34**, 1973 (1978).
[5]W. J. Crama, Ph.D. thesis, Leiden, 1980.
[6]J. García, J. Bartolomé, J. Navarro, R. Burriel, D. Gonzalez, W. J. Crama, and W. J. A. Maaskant, *Recent Developments in Condensed Matter Physics* (Plenum, New York, 1981), p. 11.
[7]J. García, J. Bartolomé, J. Navarro, D. Gonzalez, and W. J. Crama, J. Chem. Therm. **15**, 1109 (1983).
[8]W. J. Crama, M. Bakker, G. C. Verschoor, and W. J. A. Maaskant, Acta Crystallogr. B **35**, 1875 (1979).
[9]G. A. Gehring and K. A. Gehring, Rep. Prog. Phys. **38**, 1 (1975).
[10]R. Englman, *The Jahn-Teller Effect in Molecules and Crystals* (Wiley Interscience, New York, 1972).
[11]G. L. McPherson, T. J. Kistenmacher, J. B. Folkers, and G. D. Stucky, J. Chem. Phys. **57**, 3771 (1972).
[12]W. J. Crama, Acta Crystallogr. B **37**, 2133 (1981).
[13]N. W. Alcock, Ch. F. Putnik, and S. L. Holt, Inorg. Chem. **15**, 12 (1976); **15**, 3175 (1976).
[14]R. Laiho, M. Natarajan, and M. Kaira, Phys. Status Solidi **15**, 311 (1973).
[15]H. A. Graf, H. Tanaka, H. Dachs, N. Pyka, U. Schotte, and G. Shirane, Solid State Commun. **57**, 469 (1986).
[16]U. Schotte, H. A. Graf, and H. Dachs, J. Phys. Condens. Mater. **1**, 3765 (1989).
[17]H. Tanaka, K. Iio, and K. Nagata, J. Phys. Soc. Jpn. **54**, 4345 (1985).
[18]J. García, M. Benfatto, C. R. Natoli, A. Bianconi, A. Fontaine, and H. Tolentino, Chem. Phys. **132**, 295 (1989).
[19]L. G. Parratt, Rev. Mod. Phys. **31**, 616 (1959).
[20]*X-ray Absortion: Principles, Applications, Techniques of EXAFS, SEXAFS and XANES*, edited by D. C. Kronsberger and R. Prins (Wiley, New York, 1986), Chaps. I–VI. J.
[21]SERC Daresbury Laboratory EXBACK program, Warrington, United Kingdom (unpublished).
[22]S. Mobilio and A. Marcelli (unpublished).
[23]M. Sanchez del Rio and J. Chaboy (unpublished).
[24]N. Binsted, S. J. Gurman, and S. Campbell, SERC Daresbury Laboratory EXCURV88 program.
[25]P. A. Lee and J. B. Pendry, Phys. Rev. B **11**, 2795 (1975).
[26]S. J. Gurman, N. Binsted, and I. Ross, J. Phys. C **7**, 143 (1984).
[27]M. G. Aranda, J. Chaboy, and S. Bruque, Inorg. Chem. **30**, 2396 (1991).
[28]F. W. Lytle, D. E. Sayers, and E. A. Stern, Physica B **158**, 701 (1989).
[29]S. S. Hasnain, in *Biophysics and Synchrotron Radiation*, edited by A. Bianconi and A. Congiu Castellano (Springer-Verlag, Berlin, 1987).
[30]A. Chadwick, J. T. R. Dunsmuir, I. W. Forrest, A. P. Lane, and S. Fernando, J. Chem. Soc. A, p. 2794 (1971).
[31]S. Guha and J. Lange, Phys. Rev. B **15**, 4157 (1977).
[32]W. J. Crama and W. J. A. Maaskant, Physica B **121**, 219 (1983).
[33]H. Tanaka, H. Dachs, K. Iio, and K. Nagata, J. Phys. C **19**, 4861 (1986); **19**, 4879 (1986).